Z. angew. Math. Phys. 60 (2009) 450–478
0044-2275/09/030001-29
DOI 10.1007/s00033-008-7050-1
© 2008 Birkhäuser Verlag, Basel

Zeitschrift für angewandte Mathematik und Physik ZAMP

On the interaction of deep water waves and exponential shear currents

Jun Cheng, Jie Cang and Shi-Jun Liao*

Abstract. A train of periodic deep-water waves propagating on a steady shear current with a vertical distribution of vorticity is investigated by an analytic method, namely the homotopy analysis method (HAM). The magnitude of the vorticity varies exponentially with the magnitude of the stream function, while remaining constant on a particular streamline. The so-called Dubreil–Jacotin transformation is used to transfer the original exponentially nonlinear boundary-value problem in an unknown domain into an algebraically nonlinear boundary-value problem in a known domain. Convergent series solutions are obtained not only for small amplitude water waves on a weak current but also for large amplitude waves on a strong current. The nonlinear wave-current interaction is studied in detail. It is found that an aiding shear current tends to enlarge the wave phase speed, sharpen the wave crest, but shorten the maximum wave height, while an opposing shear current has the opposite effect. Besides, the amplitude of waves and fluid velocity decay over the depth more quickly on an aiding shear current but more slowly on an opposing shear current than that of waves on still water. Furthermore, it is found that Stokes criteria of wave breaking is still valid for waves on a shear current: a train of propagating waves on a shear current breaks as the fluid velocity at crest equals the wave phase speed. Especially, it is found that the highest waves on an opposing shear current are even higher and steeper than that of waves on still water. Mathematically, this analytic method is rather general in principle and can be employed to solve many types of nonlinear partial differential equations with variable coefficients in science, finance and engineering.

Keywords. Wave-current interaction, deep water waves, exponential shear current, homotopy analysis method, nonlinearity, PDE with variable coefficient.

1. Introduction

More than one century ago, Stokes [1, 2] proposed his deep water wave theory, which is nowadays known as Stokes finite amplitude wave theory and can be found in all textbooks about fluid dynamics. In the presence of the wave problem, Stokes required the fluid motion to be irrotational, supported by Lagrange theorem: when fluid starts from rest there is no vorticity anywhere, and hence the flow will remain irrotational for all time. In this paper, we shall extend Stokes nonlinear wave problem to such a case: a train of permanent deep-water waves propagates on

*The corresponding author, Email address: sjliao@sjtu.edu.cn

a steady shear current with a vertical distribution of vorticity. The magnitude of the vorticity varies exponentially with the magnitude of the stream function, while remaining constant on a particular streamline. In this case, the fluid motion is rotational. However, it has no conflict with Lagrange theorem, for we do not study the evolution of the water waves but the permanent waves on a steady nonuniform current. Hence the assumption that the water is inviscid but rotational is reasonable. In practice, waves rarely propagate on still fluid: waves that have traveled from their generation region will still encounter wind, tidal or gravity-induced flows [3]. Practically, the profile of the current is mostly exponential over the depth.

Searching for solutions of this problem has arose interests of a number of researchers in the recent half century. Due to its complex, earlier works either assume that the current is uniform, and hence ignore the effects of the vorticity distribution, or that the waves are of small amplitude and the current is weak and hence linearly sum the individual motions due to the waves and the current. In the former case, the waves can be regarded to propagate on still water in a reference frame moving with the current at the same speed, so that the uniform current can be linearly added to the pure waves. This kind of problem was investigated by Fenton [4] who derived Stokes' fifth-order solution for deep-water waves. For shallow water waves with a uniform current, Clamond [5, 6] and Clamond and Fructus [7] used the renormalization method to obtain accurate approximations. However, in practice, currents are mostly non-uniform and hence the vorticity appears. In this case, if the waves are of small amplitude or the current is weak, linear wave theory is commonly used. Contributions were made by Thompson [8], Kishida and Sobey [9] who investigated the linear shear current, Eastwood and Watson [10] who examined the bilinear current. For details, please refer to Peregrine [11], Toumazis [12] and Wang [13]. But if neither the wave amplitude is small nor the current is weak, the above mentioned methods, as can be expected, are too crude: they overestimate the waves on an aiding current but underestimate them on an opposing current.

The nonlinear theory of the wave-current interaction begins from Dalrymple [3], who numerically studied the case for a current in 1/7-power-law. Later, Thomas [14] numerically investigated the interaction of nonlinear waves and a current with exponential distribution of vorticity. Li and Chwang [15], and Wang and Li [16] used the perturbation method to give a fifth-order approximation. However, it is well-known that, in general, the perturbation approximations are valid only for weakly nonlinear problems. So, the fifth-order dispersion relationship given by the perturbation method [15, 16] is valid only for small amplitude waves on a weak current.

Currently, some analytic techniques for strongly nonlinear problems have been developed. Among them, the so-called homotopy analysis method (HAM) [17, 18, 19, 20, 21, 22] is rather attractive, which has been successfully applied to many aspects of nonlinear problems [23, 24, 25, 26, 27, 28, 29, 30, 31, 32, 33]. In the field

of the wave propagation, Liao and Cheung [19] used the homotopy analysis method to give high-order convergent series solutions for the dispersion relationship of the deep water waves. Latter, Tao and Song *et al.* [24] considered the water waves in the finite depth. By means of the *homotopy*, a simple concept in topology, the homotopy analysis method is based on a continuous variation from an initial guess to the exact solution. Thus, it is, different from the perturbation methods, independent of small physical parameters at all and thus is valid even in case of strong nonlinearity. Besides, different from all other analytic techniques, the homotopy analysis method provides us with a simple way to control and adjust the convergence of the series solutions. Further more, it provides us with great freedom to get better approximations by choosing better base functions. For details, please refer to Liao [20] and Liao and Tan [22].

The aim of this paper is to obtain accurate high-order approximations of nonlinear water waves on a shear current with exponential distribution of vorticity by means of the homotopy analysis method. The influences of the non-uniform current on the wave phase speed, the wave shape, the maximum wave height, the velocity profile and so on are investigated and discussed in detail. This paper is organized in five sections. In §2, the mathematical formulation of the wave-current interaction is given, and the Dubreil–Jacotin transformation [34, 14, 35] is introduced to reformulate the original moving boundary problem into a fixed one. In §3, the homotopy analysis method is applied to get accurate analytic approximations. The influence of the non-uniform current on the water waves is discussed in §4. Finally, a conclusion is drawn in §5.

2. Mathematical formulation

2.1. Original boundary value problem

Cartesian coordinates (x, y) are chosen so that the horizontal x-axis is in the direction of wave propagation, the y-axis points vertically upwards, and the origin lies the mean water level. When the waves exist, we shall use a moving reference frame $(x' - ct, y') \mapsto (x, y)$, where c is the wave phase speed, (x', y') is the coordinate in the still reference frame, so that the problem is steady. Let $y = \eta(x)$ denote the free surface, H the wave height, λ the wave length, $\boldsymbol{u}_w = \{u_w(x, y), v_w(x, y)\}$ the wave-induced velocity field, $\boldsymbol{u}_c = \{u_c(y), v_c(y)\}$ the current-induced velocity field and $\boldsymbol{u} = \{u(x, y), v(x, y)\}$ the whole velocity field of waves on the current, respectively. Introducing the stream function $\psi(x, y)$ defined by

$$\psi_y(x, y) = u(x, y) - c, \qquad \psi_x(x, y) = -v(x, y), \tag{1}$$

we obtain the governing equation

$$\psi_{xx} + \psi_{yy} = -\Omega(\psi), \tag{2}$$

where the subscript denotes partial derivatives and $\Omega(\psi)$ is the given vorticity distribution of the current. Consider a limiting case where there is only a current but no waves in water. We can still use equation (1) to introduce the steam function but the wave phase speed should be zero, i.e, $c = 0$. When $\Omega(\psi) = 0$, the governing equation reduces to a Laplace equation which is just the case of the Stokes water wave problem; When $\Omega(\psi)$ is a non-zero constant, it is the case for a linear shear current. In this paper, we investigate a current with vorticity, whose magnitude exponentially decays in the direction of water depth as indicated by Phillips [36], i.e. $\Omega(\psi) = \epsilon \exp(-\psi)$, where ϵ is a physical parameter determining the strength of the vorticity. Note that, when $\epsilon < 0$, the current moves in the same direction of wave propagation and is called the aiding current. When $\epsilon > 0$, the current moves in the opposing direction of wave propagation, and is called opposing current. Note that the vorticity of all uniform currents is zero. So, a given distribution of vorticity corresponds to an infinite number of currents. To avoid this, we consider here only the case that $\epsilon = 0$ corresponds to the still water.

To guarantee a unique solution, the boundary conditions should be imposed. In the infinite depth, it holds

$$\psi_x \to 0 \qquad \text{as} \qquad y \to -\infty. \tag{3}$$

On the free surface, the kinematic free-surface condition gives

$$\psi = 0 \qquad \text{on} \qquad y = \eta(x). \tag{4}$$

The dynamic free surface condition is specified as

$$\frac{1}{2}(\psi_x^2 + \psi_y^2) + g\, y = Q \qquad \text{on} \qquad y = \eta(x), \tag{5}$$

where Q is the so-called Bernoulli constant on the free surface streamline, which is unknown and need be determined.

Mathematically, it is difficult to solve the above nonlinear partial differential equations (2) to (5). For a given vorticity distribution $\Omega(\psi) = \epsilon \exp(-\psi)$, the above equations contain three unknowns: the stream function $\psi(x, y)$, the free surface $\eta(x)$, and the Bernoulli constant Q. Besides, physically speaking, the wave phase speed c is also unknown. Note that, the governing equation (2) contains the *exponential* term $\Omega(\psi) = \epsilon \exp(-\psi)$ which possesses a rather strong nonlinearity for the unknown stream-function ψ. Besides, the dynamic condition (5) of the free surface is *nonlinear* and satisfied on the *unknown* free surface boundary $y = \eta(x)$. The nonlinearity of the governing equation (2) and the boundary condition (5), and especially the unknown free surface $y = \eta(x)$, bring us great mathematical difficulties to solve this nonlinear boundary-value problem.

2.2. Dubreil–Jacotin transformation

In order to handle the unknown free surface, we use the Dubreil–Jacotin transformation [34, 14, 35] to reformulate the problem as a boundary value problem in

a *known* domain. The stream function ψ is regarded as an independent variable (like x), and y is regarded as a unknown function dependent on both x and ψ, expressed by $y(x,\psi)$. Then, according to the fundamental theorems in calculus, we have from (1) the local velocity components

$$u - c = \frac{1}{y_\psi}, \qquad v = \frac{y_x}{y_\psi}. \tag{6}$$

In fluid mechanics, it is common to adopt dimensionless variables. Here, for the case where the waves exist, the following dimensionless variables

$$x = k\, x^*, \qquad y = k\, y^*, \qquad \psi = \frac{k}{c}\, \psi^*, \qquad \Omega(\psi) = \frac{1}{k\, c}\, \Omega^*(\psi), \tag{7}$$

are introduced, where variables with asterisk are dimensional and $k = 2\pi/\lambda$ is the wave number. Thus, the problem governed by the original equations (2) to (5) in the *unknown* domain $-\infty < y \le \eta(x)$ and $-\infty < x < +\infty$ is reformulated in a *known* domain $0 \le \psi < +\infty$ and $-\infty < x < +\infty$:

$$y_{xx}\, y_\psi^2 - 2\, y_x\, y_\psi\, y_{x\psi} + (1 + y_x^2)\, y_{\psi\psi} = y_\psi^3\, \Omega(\psi), \tag{8}$$

subject to the boundary conditions

$$\delta\, (1 + y_x^2) + 2\, (y - \kappa)\ y_\psi^2 = 0 \qquad \text{on } \psi = 0, \tag{9}$$

$$y_x \to 0 \qquad \text{as } \psi \to +\infty, \tag{10}$$

where both $\delta = c^2/c_0^2$ and $\kappa = kQ/g$ are unknown constants, although $c_0^2 = g/k$ is known. So, the above equations contain three unknowns: one unknown function $y(x,\psi)$ and two unknown constants δ and κ. Besides, to guarantee a periodic solution, $y(x,\psi)$ must be a periodic function in the x direction with the period 2π. Thus, the dimensionless wave height H scaled by k^{-1} is given by

$$H = y(0,0) - y(\pi,0). \tag{11}$$

Since there should be no change in the mean water level due to the presence of the waves, i.e. $\int_0^\pi \eta(x)dx = 0$, the free surface is given by

$$\eta(x) = y(x,0) - \frac{1}{\pi}\int_0^\pi y(x,0)\, \mathrm{d}x. \tag{12}$$

So, when $y(x,\psi)$ is obtained, it is easy to get the wave surface $y = \eta(x)$.

Note that, using the Dubreil–Jacotin transformation [34, 14, 35], the original nonlinear equation (2) with exponentially nonlinear term $\Omega(\psi) = \epsilon \exp(-\psi)$ becomes the nonlinear equation (8) with the variable coefficient $\Omega(\psi) = \epsilon \exp(-\psi)$. Although equation (8) looks much more complicated than (2), its nonlinearity is actually weaker than that of equation (2), because the exponential term $\Omega(\psi) = \epsilon\ \exp(-\psi)$ in (8) is regarded now as a *known* variable coefficient. Besides, the free surface boundary conditions are now satisfied on the *known* boundary $\psi = 0$. Therefore, the use of the Dubreil–Jacotin transformation [34, 14, 35] simplifies the original problem, although equation (8) looks more complicated than (2).

3. Homotopy analysis method

In this section, the homotopy analysis method [17, 18, 19, 20, 21, 22] is employed to give the convergent series solutions of $y(x,\psi)$, δ and κ, governed by nonlinear partial differential equation (8) with variable coefficient $\Omega(\psi) = \epsilon \exp(-\psi)$, subject to the boundary conditions (9) and (10).

3.1. Solution expression

Using the homotopy analysis method, one often starts from the solution expression of the nonlinear problems under consideration. Note that, the partial differential equation (8) contains a variable coefficient $\Omega(\psi) = \epsilon\ \exp(-\psi)$ and only one linear term $y_{\psi\psi}$, therefore, is highly nonlinear. Mathematically, from this rather complicated nonlinear equation, it seems impossible to guess the expression form of the solution $y(x,\psi)$. However, considering the physical background of the considered problem, it is easy for us to find a proper solution expression of it. Physically speaking, in the moving reference frame, the problem is composed of a train of deep-water waves, a uniform current caused by the motion of the reference frame, and a non-uniform current possessing an exponential distribution of vorticity. Obviously, in case of the pure deep-water waves ($\Omega = 0$), the periodic wave elevation is expressed by

$$y = \sum_{m=0}^{+\infty} a_m\ \cos(mx),$$

where a_m is a constant coefficient. In case of a non-uniform current with vorticity distribution $\Omega = \epsilon \exp(-\psi)$, equation (8) contains the term $\exp(-\psi)$, therefore, it is straightforward that $y(x,\psi)$ should contain the term $\exp(-n\psi)$, where $n \geq 1$ is an integer. Besides, wave elevation is still periodic in the x direction, thus $y(x,\psi)$ should contain the term $\cos(mx)$. Furthermore, it is well-known that the uniform current due to the motion of the reference frame won't give rise to the wave-current interaction. Therefore, from viewpoints of the physical considerations mentioned above, even without solving the nonlinear partial differential equations (8) to (11), we clearly know that $y(x,\psi)$ should be expressed in the following form

$$y = -\psi + \sum_{n=1}^{+\infty} \sum_{m=0}^{+\infty} \alpha_{n,m}\ \exp(-n\psi)\ \cos(mx), \tag{13}$$

where the first part results from the uniform current due to the motion of the reference frame, and the second part from the combined effect of the waves and the current. The above formula provides us the so-called *solution expression* of $y(x,\psi)$, which plays an important role in the frame of the homotopy analysis method, as shown later. Note that this solution expression *automatically* satisfies the boundary condition (10).

3.2. Continuous variation

The homotopy analysis method is based on a kind of continuous variation (or deformation) from an initial guess to the exact solution. For the sake of simplicity, we first define, according to equations (8) and (9), the following nonlinear operators

$$\mathcal{N}_g\,[\,Y(x,\psi;q)\,] = Y_{xx}\,Y_\psi^2 - 2\,Y_x\,Y_{x\psi}Y_\psi + (1+Y_x^2)\,Y_{\psi\psi} - \Omega\,Y_\psi^3, \tag{14}$$

$$\mathcal{N}_b\,[Y(x,\psi;q),\ \Delta(q),\ \Gamma(q)\,] = \Delta\,\left(\,1+Y_x^2\,\right) + 2\,(\,Y-\Gamma\,)\,Y_\psi^2, \tag{15}$$

for the governing equation (8) and the boundary condition (9), respectively, where $q \in [0,1]$ denotes the embedding parameter (or called homotopy parameter). We construct the continuous maps (or deformations) $Y(x,\psi;q) \mapsto y(x,\psi)$, $\Delta(q) \mapsto \delta$ and $\Gamma(q) \mapsto \kappa$ such that, as q increases from 0 to 1, $Y(x,\psi;q)$, $\Delta(q)$ and $\Gamma(q)$ vary continuously from the initial guess $y_0(x,\psi)$, δ_0 and κ_0 to the exact solution $y(x,\psi)$, δ and κ, respectively. Such kind of continuous maps (or variations) can be defined by the so-called zeroth-order deformation equations

$$(1-q)\,\mathcal{L}_g\,[\,Y(x,\psi;q) - y_0(x,\psi)\,] = \hbar\,q\,\mathcal{N}_g[\,Y(x,\psi;q)\,], \tag{16}$$

subject to the boundary conditions

$$(1-q)\mathcal{L}_b\,[Y(x,\psi;q) - y_0(x,\psi)] = \hbar q \mathcal{N}_b[\,Y(x,\psi;q),\Delta(q),\Gamma(q)] \text{ on } \psi = 0, \tag{17}$$

$$\frac{\partial Y(x,\psi;q)}{\partial x} = 0 \quad \text{as} \quad \psi \to +\infty, \tag{18}$$

with the definition of the wave height

$$Y(0,0;q) - Y(\pi,0;q) = H, \tag{19}$$

where $\hbar$ is a nonzero auxiliary parameter, $y_0(x,\psi)$ is an initial guess of $y(x,\psi)$, $\mathcal{L}_g$ and $\mathcal{L}_b$ are two auxiliary linear operators, respectively. The auxiliary linear operators $\mathcal{L}_g$ and $\mathcal{L}_b$ have the property $\mathcal{L}_g[0] = 0$ and $\mathcal{L}_b[0] = 0$, and will be chosen later. Obviously, when $q = 0$, the zeroth-order deformation equations (16) to (19) give rise to

$$Y(x,\psi;0) = y_0(x,\psi), \qquad \Delta(0) = \delta_0, \qquad \Gamma(0) = \kappa_0, \tag{20}$$

where δ_0 and κ_0 are the initial solutions of δ and κ, respectively, which will be determined later. When $q = 1$, since $\hbar \neq 0$, the zeroth-order deformation equations (16) to (19) are equivalent to the original equations (8) to (11), provided

$$Y(x,\psi;1) = y(x,\psi), \qquad \Delta(1) = \delta, \qquad \Gamma(1) = \kappa. \tag{21}$$

Hence, as the homotopy-parameter q increases from 0 to 1, $Y(x,\psi;q), \Delta(q)$ and $\Gamma(q)$ indeed vary from the initial guess $y_0(x,\psi)$, δ_0 and κ_0 to the exact solutions $y(x,\psi)$, δ and κ, respectively. Such kind of continuous variations are called deformation in topology: this is the reason why equations (16) to (19) are called zeroth-order deformation equations.

It should be emphasized that, using the homotopy analysis method, one has great freedom to choose the auxiliary linear operators and the initial guess under

some basic rules (please refer to Liao [20, 22]). Note that equation (8) contains only one linear term $y_{\psi\psi}$. However, if we choose $\mathcal{L}_g u = u_{\psi\psi}$ as the auxiliary linear operator, we would get a solution $y(x, \psi)$ in power series of ψ, which obviously can not satisfy the boundary condition (10). So, the linear term of equation (8) might greatly mislead us, as illustrated by Liao [22] for some other examples. Fortunately, the homotopy analysis method provides us with great freedom to choose the auxiliary linear operators, so that we can completely forget the linear term $y_{\psi\psi}$ in equation (8) and choose proper auxiliary linear operators $\mathcal{L}_g$ and $\mathcal{L}_b$ by means of the solution expression (13) that is obtained under the physical considerations. Note that $u = \exp(-\psi)\cos(x)$ satisfies

$$\frac{\partial^2 u}{\partial \psi^2} + \frac{\partial^2 u}{\partial x^2} = 0.$$

So, to obey the solution expression (13), we choose the following auxiliary linear operator

$$\mathcal{L}_g u = \frac{\partial^2 u}{\partial \psi^2} + \frac{\partial^2 u}{\partial x^2}. \tag{22}$$

Similarly, the boundary condition (9) does not contain any linear terms. Fortunately, we also have great freedom to choose the auxiliary linear operator $\mathcal{L}_b$, too. To obey the solution expression (13), we choose the following auxiliary linear operator

$$\mathcal{L}_b u = u + \frac{\partial u}{\partial \psi} \tag{23}$$

for the nonlinear boundary condition (9). Here, it should be emphasized that the above two auxiliary linear operators (22) and (23) have nearly no relationships with the governing equation (8) and the boundary condition (9), respectively! This is mainly because the homotopy analysis method provides us with great freedom to choose the auxiliary linear operators $\mathcal{L}_g$ and $\mathcal{L}_b$ according to the solution expression (13) that is obtained under the physical considerations. This kind of freedom is an obvious advantage of the homotopy analysis method over other analytic techniques, and can greatly simplify the process of solving nonlinear problems, as illustrated by Liao [22].

Besides, the homotopy analysis method also provides us with great freedom to choose the initial guess. As mentioned before, the initial guess $y_0(x, \psi)$ should satisfy the solution expression (13) and the definition of wave height (11). So, it is straightforward for us to choose such an initial guess

$$y_0(x, \psi) = -\psi + \frac{H}{2}\exp(-\psi)\ \cos x. \tag{24}$$

Note that the initial solutions δ_0 and κ_0 are still unknown right now and will be determined later.

3.3. High-order deformation equation

By Taylor's theorem and using equation (20), we expand $Y(x, y; q)$, $\Delta(q)$ and $\Gamma(q)$ into the Taylor series about the homotopy-parameter q:

$$Y(x, \psi; q) = y_0(x, \psi) + \sum_{n=1}^{+\infty} y_n(x, \psi)\, q^n, \tag{25}$$

$$\Delta(q) = \delta_0 + \sum_{n=1}^{+\infty} \delta_n\, q^n, \tag{26}$$

$$\Gamma(q) = \kappa_0 + \sum_{n=1}^{+\infty} \kappa_n\, q^n, \tag{27}$$

where

$$y_n(x, \psi) = \frac{1}{n!} \frac{\partial^n Y(x, \psi; q)}{\partial q^n}\bigg|_{q=0}, \quad \delta_n = \frac{1}{n!} \frac{\partial^n \Delta(q)}{\partial q^n}\bigg|_{q=0}, \quad k_n = \frac{1}{n!} \frac{\partial^n \Gamma(q)}{\partial q^n}\bigg|_{q=0}.$$

It is well-known that a Taylor series has often finite convergence radius. Fortunately, we introduce the non-zero auxiliary parameter $\hbar$ in the zeroth-order deformation equations (16) and (17), which can be used to adjust and control the convergence radius of the above series, as shown by Liao [17, 18, 19, 20, 21, 22] and others [23, 24, 25, 26, 27, 28, 29, 30, 31, 32, 33]. Assuming that the auxiliary parameter $\hbar$ is so properly chosen that the above three series are convergent at $q = 1$, we have the series solution

$$y(x, \psi) = y_0(x, \psi) + \sum_{n=1}^{+\infty} y_n(x, \psi), \tag{28}$$

$$\delta = \delta_0 + \sum_{n=1}^{+\infty} \delta_n, \tag{29}$$

$$\kappa = \kappa_0 + \sum_{n=1}^{+\infty} \kappa_n. \tag{30}$$

The governing equation and boundary conditions of the unknown $y_n(x, \psi)$ can be deduced uniquely from the zeroth-order deformation equations (16) to (19). For simplicity, define the vectors

$$\begin{aligned} \boldsymbol{y}_n &= \{\, y_0,\ y_1,\ y_2,\ \cdots,\ y_n \,\}, \\ \boldsymbol{\delta}_n &= \{\, \delta_0,\ \delta_1,\ \delta_2\ ,\cdots,\ \delta_n \,\}, \\ \boldsymbol{\kappa}_n &= \{\, \kappa_0,\ \kappa_1,\ \kappa_2,\ \cdots,\ \kappa_n \,\}. \end{aligned} \tag{31}$$

Directly substituting the series (25) to (27) into the zeroth-order deformation equations (16) to (19), equating the coefficients of the like-power of q, we obtain

the nth-order deformation equations ($n \geq 1$):

$$\mathcal{L}_g\left(\, y_n - \chi_n \, y_{n-1} \,\right) = \hbar \, R_n\left(\boldsymbol{y}_{n-1}\right), \tag{32}$$

subject to the boundary conditions

$$\mathcal{L}_b\left(\, y_n - \chi_n \, y_{n-1} \,\right) = \hbar \, S_n\left(\boldsymbol{y}_{n-1}, \boldsymbol{\kappa}_{n-1}, \boldsymbol{\delta}_{n-1}\right) \qquad \text{on} \;\; \psi = 0, \tag{33}$$

$$\frac{\partial y_n}{\partial x} = 0 \quad \text{as} \quad \psi \to +\infty, \tag{34}$$

under the restriction

$$y_n(0,0) - y_n(\pi,0) = 0, \tag{35}$$

where χ_k is a unit step function defined by

$$\chi_k = \begin{cases} 0, \; k \leq 1, \\ 1, \; k > 1, \end{cases} \tag{36}$$

and

$$\begin{aligned} R_n = {} & \sum_{i=0}^{n-1} \frac{\partial^2 y_{n-1-i}}{\partial x^2} \sum_{j=0}^{i} \frac{\partial y_{i-j}}{\partial \psi} \frac{\partial y_j}{\partial \psi} - 2 \sum_{i=0}^{n-1} \frac{\partial y_{n-1-i}}{\partial x} \sum_{j=0}^{i} \frac{\partial^2 y_{i-j}}{\partial x \partial \psi} \frac{\partial y_j}{\partial \psi} + \frac{\partial^2 y_{n-1}}{\partial \psi^2} \\ & + \sum_{i=0}^{n-1} \frac{\partial^2 y_{n-1-i}}{\partial \psi^2} \sum_{j=0}^{i} \frac{\partial y_{j-i}}{\partial x} \frac{\partial y_i}{\partial x} - \Omega(\psi) \sum_{i=0}^{n-1} \frac{\partial y_{n-1-i}}{\partial \psi} \sum_{j=0}^{i} \frac{\partial y_{j-i}}{\partial \psi} \frac{\partial y_i}{\partial \psi}, \end{aligned} \tag{37}$$

$$\begin{aligned} S_n = {} & \delta_{n-1} + \sum_{i=0}^{n-1} \delta_{n-1-i} \sum_{j=0}^{i} \frac{\partial y_{i-j}}{\partial x} \frac{\partial y_j}{\partial x} \\ & + 2 \sum_{i=0}^{n-1} \left(y_{n-1-i} - \kappa_{n-1-i}\right) \sum_{j=0}^{i} \frac{\partial y_{i-j}}{\partial \psi} \frac{\partial y_j}{\partial \psi}. \end{aligned} \tag{38}$$

Note that, for the nth-order deformation equation, the righthand-side terms R_n and S_n are dependent upon $\boldsymbol{y}_{n-1}, \boldsymbol{\delta}_{n-1}$ and $\boldsymbol{\kappa}_{n-1}$, and therefore are regarded as known terms. So, according to the definitions (22) and (23), the high-order deformation equation (32) is *linear* with *constant* coefficients, subject to the *linear* boundary conditions (33) and (34) on the *known* boundary $\psi = 0$. Such kind of linear boundary-value problem in a fixed domain is easy to solve, as shown in the coming subsection. Therefore, by means of the homotopy analysis method, the original nonlinear partial differential equation with variable coefficient is transferred into an infinite number of linear partial differential equations with *constant* coefficients.

3.4. Successive solution procedure

Note that the nth-order deformation equations (32) to (35) contain three unknowns: $y_n(x,\psi)$, δ_{n-1} and κ_{n-1}. Due to the definition (22) of the auxiliary

linear operator $\mathcal{L}_g$, it holds for any positive integer M that

$$\mathcal{L}_g\left[\sum_{m=1}^{M} C_{n,m}\ \exp(-m\psi)\cos(mx)\right] = 0,$$

where $C_{n,m}$ is a constant. Thus, the general solution of the high-order deformation equation (32) is

$$y_n(x,\psi) = \chi_n\ y_{n-1}(x,\psi)\ + y_n^*(x,\psi) + \sum_{m=1}^{M} C_{n,m}\ \exp(-m\psi)\cos(mx), \quad (39)$$

where M is a positive integer to be determined, and

$$y_n^*(x,\psi)\ =\ \hbar\ \mathcal{L}_g^{-1}\left[\ R_n(\boldsymbol{y}_{n-1})\ \right] \quad (40)$$

is a special solution of $y_n(x,\psi)$, in which $\mathcal{L}_g^{-1}$ is an inverse operator of $\mathcal{L}_g$, defined by

$$\begin{aligned}
\mathcal{L}_g^{-1}\left[\exp(-m\psi)\cos(nx)\right] &= \frac{\exp(-m\psi)\cos(nx)}{(m^2-n^2)},\\
\mathcal{L}_g^{-1}\left[\exp(-m\psi)\sin(nx)\right] &= \frac{\exp(-m\psi)\sin(nx)}{(m^2-n^2)}, \qquad (m\neq n).
\end{aligned} \quad (41)$$

In this way, it is easy to get the special solution $y_n^*(x,\psi)$, especially by means of the symbolic computation software such as Mathematica, Maple and so on.

To determine the unknown δ_{n-1}, κ_{n-1} and $C_{n,m}$, we substitute the expression (39) into the boundary condition (33), i.e.

$$\mathcal{L}_b\left[\sum_{m=1}^{M} C_{n,m}\ \exp(-m\psi)\cos(mx)\right] = -\mathcal{L}_b(\ y_n^*\ ) + \hbar\ S_n\left(\boldsymbol{y}_{n-1}, \boldsymbol{\kappa}_{n-1}, \boldsymbol{\delta}_{n-1}\right) \quad \text{on}\ \ \psi = 0. \quad (42)$$

It is found that the above equation can be expressed by

$$\sum_{m=2}^{M}(1-m)\ C_{n,m}\ \cos(mx) = \sum_{m=0}^{2n+1}\ \gamma_{n,m}(\boldsymbol{\kappa}_{n-1}, \boldsymbol{\delta}_{n-1})\ \cos(mx), \quad (43)$$

where the expression of $\gamma_{n,m}(\boldsymbol{\kappa}_{n-1}, \boldsymbol{\delta}_{n-1})$ is known. Balancing both sides of the above equation, we have

$$M = 2n+1, \qquad C_{n,m} = \frac{\gamma_{n,m}(\boldsymbol{\kappa}_{n-1}, \boldsymbol{\delta}_{n-1})}{(1-m)}, \quad 1 < m \leq 2n+1,$$

and

$$\gamma_{n,0}(\boldsymbol{\kappa}_{n-1}, \boldsymbol{\delta}_{n-1}) = 0, \qquad \gamma_{n,1}(\boldsymbol{\kappa}_{n-1}, \boldsymbol{\delta}_{n-1}) = 0, \quad (44)$$

which just provide us the two algebraic equations to determine the unknown κ_{n-1} and δ_{n-1}.

Up to now, only $C_{n,1}$ is unknown. Substituting the expression (39) into equation (35) gives

$$y_n^*(0,0) - y_n^*(\pi,0) + \sum_{m=1}^{2n+1} C_{n,m} - \sum_{m=1}^{2n+1} C_{n,m}\ \cos(m\pi) = 0. \tag{45}$$

Therefore,

$$C_{n,1} = -\frac{1}{2}\left\{ y_n^*(0,0) - y_n^*(\pi,0) + \sum_{m=2}^{2n+1} [1-(-1)^m]\, C_{n,m} \right\}. \tag{46}$$

Hence, all unknowns are determined and thus the problem is closed. Note that all of the above computations can be done by means of symbolic computation software, and thus $y_n(x,\psi)$, δ_{n-1} and κ_{n-1} can be obtained successively in order $n = 1, 2, 3$ and so on. For example, solving the 1st-order deformation equations, we have

$$\kappa_0 = \frac{1}{320}\,(160 + 25\ H^2 + 80\ \epsilon + 3\ \epsilon\ H^2), \tag{47}$$

$$\delta_0 = \frac{1}{8+H^2}\ \left(8 - \frac{3}{4}H^2 + \frac{5}{32}\ H^4 + 4\epsilon - \frac{1}{60}\ \epsilon\ H^2 + \frac{3}{160}\ \epsilon\ H^4 \right) \tag{48}$$

and

$$y_1(x,\psi) = \hbar\,[A_{1,0}(\psi) + A_{1,1}(\psi)\cos x + A_{1,2}(\psi)\cos 2x + A_{1,3}(\psi)\cos 3x]\,, \tag{49}$$

where

$$\begin{aligned}
A_{1,0}(\psi) &= -\frac{H^2}{8}\exp(-2\psi) + \epsilon\exp(-\psi) + \frac{\epsilon H^2}{24}\exp(-3\psi),\\
A_{1,1}(\psi) &= \frac{3H^3}{64}\exp(-\psi) - \frac{H^3}{64}\exp(-3\psi) - \frac{\epsilon H}{2}\exp(-\psi)\\
&\quad -\frac{9\epsilon H^3}{2240}\exp(-\psi) + \frac{\epsilon H}{2}\exp(-2\psi) + \frac{\epsilon H^3}{160}\exp(-4\psi),\\
A_{1,2}(\psi) &= -\frac{H^2(256+40H^2-5H^4)}{128(8+H^2)}\exp(-2\psi)\\
&\quad -\frac{\epsilon H^2(384+136H^2-9H^4)}{1920(8+H^2)}\exp(-2\psi) + \frac{3\epsilon H^2}{40}\exp(-3\psi),\\
A_{1,3}(\psi) &= -\frac{H^3}{32}\exp(-3\psi) - \frac{3\epsilon H^3}{448}\exp(-3\psi) + \frac{\epsilon H^3}{224}\exp(-4\psi).
\end{aligned}$$

Similarly, we can obtain $\kappa_1, \delta_1, y_2(x,\psi)$, and so on. It is found that all of our solutions $y_n(x,\psi)$ contain the term $\exp(-m\psi)$, where $m \geq 1$, so that the boundary condition (34) is automatically satisfied. As long as the convergent series solution of $y(x,\psi)$ is obtained, one can get the velocity field by (6) and the wave surface by (12). The wave phase speed c^2/c_0^2 is given by δ. And the energy on the stream line is given by κ.

It is found that $y(x,\psi)$ can be expressed by

$$y(x,\psi) = y_c(\psi) + y_w(x,\psi) + y_i(x,\psi),$$

where

$$y_c(\psi) = y(x,\psi)|_{H=0}$$

is the solution for the pure current without waves,

$$y_w(x,\psi) = y(x,\psi)|_{\epsilon=0}$$

is the solution for the pure waves without the current, and $y_i(x,\psi)$ denotes the solution related to wave-current interaction. Similarly, the velocity field is composed of three parts caused by the pure current, the pure wave and the wave-current interaction, respectively.

4. Results analysis

Except where the waves do not exist (in case of the pure current), the velocity field discussed in this section is scaled by the phase speed c and the wave height H is scaled by $1/k$, respectively.

Different from approximations given by perturbation methods or other non-perturbation techniques, our series solutions (28), (29) and (30) contain the auxiliary parameter $\hbar$, which provides us with a simple way to control and adjust the convergence of the series solution, as shown by Liao [17, 18, 19, 20, 21, 22] and others [23, 24, 25, 26, 27, 28, 29, 30, 31, 32, 33]. However, physically speaking, the wave phase speed c and the wave surface $\eta(x)$ are dependent upon the physical parameters H and ϵ only, having nothing to do with the auxiliary parameter $\hbar$. Thus, for given H and ϵ, from the physical point of view, all convergent series solutions (29) given by different values of $\hbar$ should converge to the same value of δ, so do all convergent series solutions (30) to the same value of κ. Mathematically, this is indeed true, as proved by Liao [20] in rather general cases. Thus, we can choose a proper value of the auxiliary parameter $\hbar$ by plotting the so-called $\hbar$-curves, such as $\delta \sim \hbar$ and $\kappa \sim \hbar$, in which one regards $\hbar$ as an independent variable and δ or κ as its function. For example, the curve of $\delta \sim \hbar$ at the 10th-order approximation in case of $H = 0.3$ and $\epsilon = 0.2$ is shown in Fig. 1. It is seen that there is an almost horizontal regime within $-0.8 < \hbar < -0.2$, which indicates the valid region of $\hbar$: any values of $\hbar$ within this region ensures the convergence of the series solutions of δ. It is found that the corresponding series of κ and $y(x,\psi)$ are also convergent within $-0.8 < \hbar < -0.2$. So, by means of the so-called $\hbar$ curves, one can find a proper value of $\hbar$ to ensure the convergence of the solution series δ, κ and $y(x,\psi)$.

There is another way to obtain high-order convergent approximations. It is the so-called homotopy-Padé technique [20], which can not only greatly accelerate the convergence of the series solution, but also eliminate the auxiliary parameter $\hbar$ from the solutions series for the considered problem. That is to say we can always

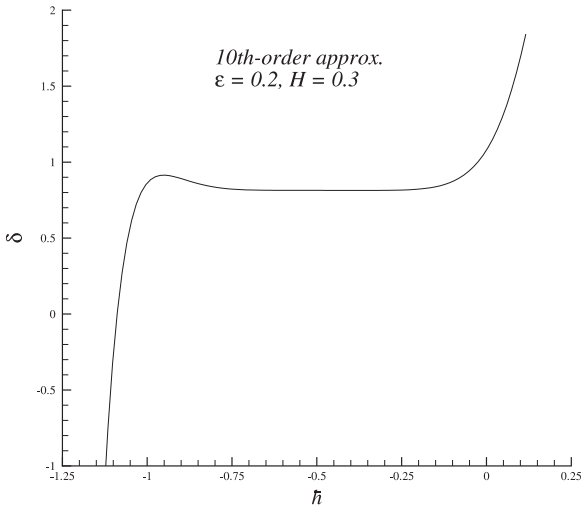

Figure 1. The curve $\delta \sim \hbar$ at the 10th-order of approximation in case of $H = 0.3$ and $\epsilon = 0.2$.

obtain convergent homotopy-Padé approximations even if the series solutions are divergent due to the improper choice of $\hbar$. For details about the homotopy-Padé technique, please refer to Liao [20, 21]. In this paper, we shall use both methods to obtain convergent solutions.

Table 1. The $[m, m]$ homotopy-Padé approximation of c^2/c_0^2 for deep-water waves on still water ($\epsilon = 0$)

H	[15,15]	[17,17]	[19,19]	[20,20]	[21,21]
0.65	1.1113	1.1113	1.1113	1.1113	1.1113
0.70	1.1300	1.1300	1.1300	1.1300	1.1300
0.75	1.1502	1.1502	1.1502	1.1502	1.1502
0.80	1.1712	1.1712	1.1712	1.1712	1.1712
0.85	1.1905	1.1904	1.1905	1.1904	1.1904
0.86	1.1926	1.1929	1.1930	1.1930	1.1930
0.87	1.1939	1.1940	1.1941	1.1941	1.1941
0.875	1.1933	1.1932	1.1936	1.1936	1.1936
0.88	1.1915	1.1909	1.1917	1.1916	1.1916
0.882	1.1902	1.1892	1.1902	1.1902	1.1902
0.8825	1.1898	1.1887	1.1898	1.1898	1.1897

Before discussing the wave-current interaction, let us consider the two limiting cases first: the pure water wave case and the pure current case. When $\Omega = 0$, it is the Stokes deep water wave model [1]. According to Stokes' theory [37], a train of propagating deep-water waves breaks when the wave height arrives at its maximum value $H = 0.886$, corresponding to the maximum crest angle $\alpha = 120$ degree. It

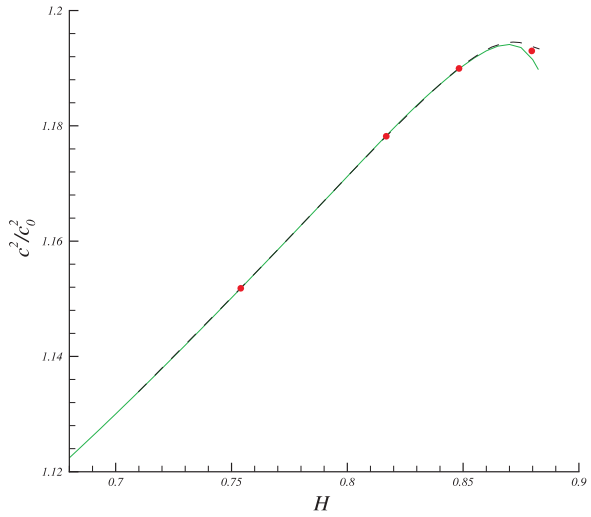

Figure 2. Comparison of the dispersion relationship of pure deep water waves. Solid line, [23,23] homotopy-Padé approximation; Dashed-line: Longuet-Higgins's result [39]; Symbols: Schwartz's result [38].

Table 2. The $[m, m]$ homotopy-Padé approximation of the crest elevation η_c for deep-water waves on still water ($\epsilon = 0$) and a comparison with $H/2$.

H	[15,15]	[17,17]	[19,19]	[20,20]	1-$H/(2\eta_c)$
0.65	0.3875	0.3875	0.3875	0.3875	16.13%
0.7	0.4250	0.4250	0.4250	0.4250	17.65%
0.75	0.4649	0.4649	0.4649	0.4649	19.34%
0.8	0.5080	0.5079	0.5079	0.5079	21.24%
0.85	0.5566	0.5566	0.5565	0.5565	23.63%
0.86	0.5675	0.5672	0.5672	0.5671	24.18%
0.87	0.5793	0.5805	0.5798	0.5800	25.00%
0.875	0.5855	0.5858	0.5856	0.5858	25.32%
0.88	0.5923	0.5922	0.5922	0.5922	25.70%
0.882	0.5952	0.5953	0.5949	0.5949	25.87%
0.8825	0.5956	0.5956	0.5956	0.5956	25.93%

is found that, even for the waves with large wave-amplitude close to the limiting wave, our $[m, m]$ homotopy-Padé approximations of c^2/c_0^2 and the crest elevation $\eta_c = \eta(0)$ converge as m increases, as shown in Tables 1 and 2. A comparative error of η_c with the linear estimated crest elevation $\eta_c \approx H/2$ is calculated at the last column in Table 2. For large amplitude waves, the comparative error between these two results is around 25%, which is rather big. Also, we compare our homotopy-Padé approximation of the wave phase speed with some previous results, as shown in Fig. 2. It is seen that our $[23, 23]$ homotopy-Padé approximation of c^2/c_0^2 agrees with Schwartz [38] and Longuet–Higgins [39], which indicates the validity of our

Table 3. The maximum wave height of propagating waves on a current with vorticity $\Omega = \epsilon \exp(-\psi)$.

ϵ	The maximum wave height
-0.25	0.67
0	0.8825
0.25	1.04
0.50	1.17

analytic approach from one limiting case. Note that, as shown in Tables 1 and 2, the maximum wave height given by our approach is about $H = 0.8825$, which is a little less than $H = 0.886$ given by Stokes theory [37].

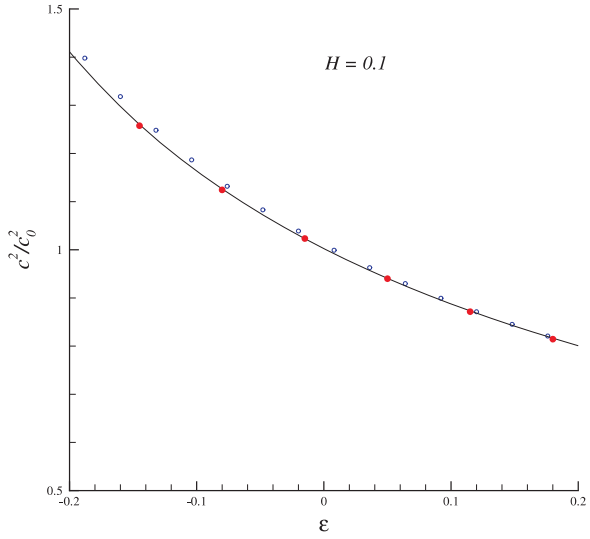

Figure 3. The influence of the vorticity parameter ϵ on the phase velocity c^2/c_0^2 of deep-water waves of $H = 0.1$. Solid line: $[2, 2]$ homotopy-Padé approximation; Dotted line: $[8, 8]$ homotopy-Padé approximation; Circle: the 5th-order perturbation solution [16].

When $H = 0$, it is the case of the pure current without waves. Obviously, it is no need to use the moving coordinates. Also, there is no wave phase speed in this case. Hence, the stream function here is defined by $u_c = \psi_y$. Since the dimensional form and the non-dimensional form of the equation (8) are the same, we can regard the solutions of this case to be dimensional. When $\hbar = -1$, our

fifth-order series solution of the pure current gives

$$y(\psi) = -\psi - \exp(-\psi)\,\epsilon + \frac{3}{4}\,\exp(-2\psi)\,\epsilon^2 - \frac{5}{6}\,\exp(-3\psi)\,\epsilon^3 + \frac{35}{32}\exp(-4\psi)\,\epsilon^4 - \frac{63}{40}\,\exp(-5\psi)\,\epsilon^5 + \text{const.} \tag{50}$$

Using the governing equation (2), we can obtain the velocity profile of the pure current in the still coordinates

$$u_c(\psi) = -\exp(-\psi)\,\epsilon + \frac{1}{2}\,\exp(-2\psi)\,\epsilon^2 - \frac{1}{2}\exp(-3\psi)\,\epsilon^3 + \frac{5}{8}\,\exp(-4\psi)\,\epsilon^4 - \frac{7}{8}\,\exp(-5\psi)\,\epsilon^5 + \frac{21}{16}\,\exp(-6\psi)\,\epsilon^6, \tag{51}$$

which is exactly the same as the perturbation solution [15], hence indicating the validity of our analytic approach from another limiting case.

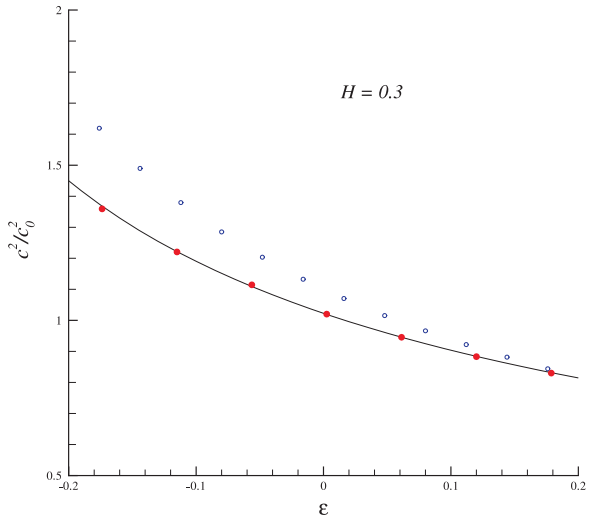

Figure 4. The influence of the vorticity parameter ϵ on the phase velocity c^2/c_0^2 of deep-water waves of $H = 0.3$. Solid line: $[2,2]$ homotopy-Padé approximation; Dotted line: $[8,8]$ homotopy-Padé approximation; Circle: the 5th-order perturbation solution [16].

The general cases of $\epsilon \neq 0$ and $H \neq 0$ are of our most interest. Our $[2,2]$ homotopy-Padé approximation of the wave phase speed is given by

$$c^2/c_0^2 = \frac{\sum_{i=0}^{8} \alpha_i(H)\epsilon^i}{1 + \sum_{j=0}^{8} \beta_j(H)\epsilon^j}, \tag{52}$$

where

$$\begin{aligned}
\alpha_0 &= 1 - 18.3545H^2 - 19.0783H^4 - 9.5071H^6 - 1.6706H^8 \\
&\quad - 0.1686H^{10} - 0.3944H^{12} + 0.1497H^{14}, \\
\alpha_1 &= -19.8095H^{-2} + 94.9902 + 79.8629H^2 + 49.2679H^4 + 16.4719H^6 \\
&\quad + 1.3127H^8 + 0.7249H^{10} - 0.5257H^{12}, \\
\alpha_2 &= -0.8127H^{-4} - 153.8798H^{-2} - 17.4780 + 8.4334H^2 - 5.1748H^4 \\
&\quad - 4.1199H^6 - 2.9438H^{10} + 0.7047H^{10}, \\
\alpha_3 &= 6.6032H^{-4} - 161.7258H^{-2} - 95.2033 - 20.2378H^2 + 3.0971H^4 \\
&\quad + 2.7794H^6 - 1.2655H^8 + 0.8404H^{10}, \\
\alpha_4 &= 5.2780H^{-4} - 79.0493H^{-2} - 48.4005 - 17.5988H^2 - 5.1302H^4 \\
&\quad + 0.4472H^6 + 0.4421H^8 + 0.0306H^{10}, \\
\alpha_5 &= 5.9728H^{-4} - 28.6492H^{-2} - 22.03866 - 3.7271H^2 + 3.03746H^4 \\
&\quad + 2.7544H^6 + 0.9785H^8 - 0.1480H^{10}, \\
\alpha_6 &= 0.4561H^{-4} - 4.9730H^{-2} - 6.5921 - 4.9442H^2 - 2.6846H^4 \\
&\quad - 0.9577H^6 - 0.2226H^8 + 0.0393H^{10}, \\
\alpha_7 &= -1.0606H^{-4} - 2.26127H^{-2} - 2.5945 - 1.6613H^2 - 0.6098H^4 \\
&\quad - 0.1298H^6 - 0.01597H^8 + 0.0014H^{10}, \\
\alpha_8 &= 0.4849H^{-4} + 1.2882H^{-2} + 1.1771 + 0.5258H^2 + 0.1341H^4 \\
&\quad + 0.0232H^6 + 0.0034H^8 + 0.0004H^{10},
\end{aligned}$$

and

$$\begin{aligned}
\beta_0 &= -18.6152H^2 - 14.3027H^4 - 4.7494H^6 + 0.3693H^8 \\
&\quad - 0.1756H^{10} - 0.6505H^{12} - 0.1882H^{14}, \\
\beta_1 &= -19.8095H^{-2} + 101.3902 + 30.9370H^2 + 5.9367H^4 - 1.9934H^6 \\
&\quad + 0.5200H^8 + 3.2108H^{10} + 1.2336H^{12}, \\
\beta_2 &= -0.8127H^{-4} - 180.3940H^{-2} + 152.2704 + 118.3418H^2 + 26.6539H^4 \\
&\quad - 5.0904H^6 - 9.6998H^8 - 3.3617H^{10}, \\
\beta_3 &= 5.5196H^{-4} - 364.0214H^{-2} - 98.3501 + 54.1467H^2 + 29.9964H^4 \\
&\quad + 5.5684H^6 - 1.2260H^8 - 0.4686H^{10}, \\
\beta_4 &= 14.4435H^{-4} - 241.5237H^{-2} - 201.5196 - 46.7589H^2 + 12.6025H^4 \\
&\quad + 11.9062H^6 + 2.9939H^8 + 0.1049H^{10}, \\
\beta_5 &= 10.2959H^{-4} - 54.8513H^{-2} - 80.1939 - 46.4665H^2 - 13.8617H^4 \\
&\quad - 1.5235H^6 + 0.18215H^8 + 0.0065H^{10}, \\
\beta_6 &= 6.7965H^{-4} + 6.2383H^{-2} - 5.5078 - 9.7100H^2 - 5.4381H^4 \\
&\quad - 1.4762H^6 - 0.17256H^8 - 0.0018H^{10}, \\
\beta_7 &= 1.28H^{-4} + 6.4458H^{-2} + 7.2395 + 3.6241H^2 + 0.9258H^4
\end{aligned}$$

$$+\ 0.1129H^6 + 0.0041H^8 - 0.0002H^{10},$$

$$\beta_8 = -1.2567H^{-4} - 1.6932H^{-2} - 0.9140 - 0.2487H^2 - 0.0366H^4 - 0.0037H^6 - 0.0006H^8.$$

As shown in Figs. 3 to 5, the above $[2,2]$ homotopy-Padé approximation agrees well with the $[8,8]$ homotopy-Padé approximation, which indicates not only the accuracy of the formula (52) but also the convergence of our series solution for waves with large amplitude. It should be emphasized that the fifth-order perturbation results given in [16] are valid only for waves with small amplitude (such as $H = 0.1$) and become more and more inaccurate with the increase of the wave height H, as shown in Figs. 3 to 5. Thus, for large wave height ($H \geq 0.3$), perturbation approximations often overestimate the wave phase speed for both aiding and opposing currents.

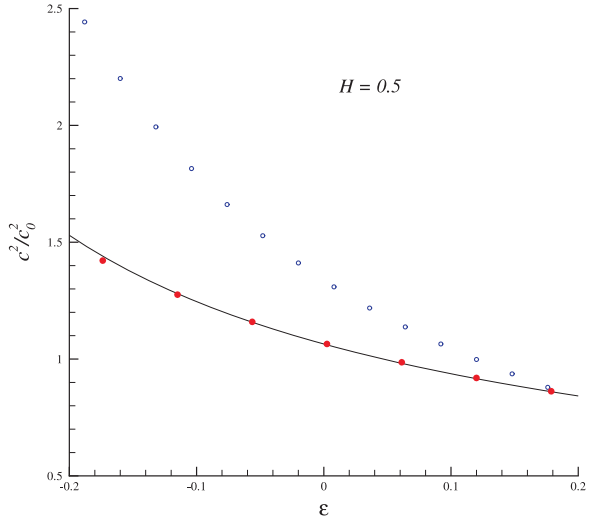

Figure 5. The influence of the vorticity parameter ϵ on the phase velocity c^2/c_0^2 of deep-water waves of $H = 0.5$. Solid line: $[2,2]$ homotopy-Padé approximation; Dotted line: $[8,8]$ homotopy-Padé approximation; Circle: the 5th-order perturbation solution [16].

Given ϵ, one can get the dispersion relationship in a similar way as that for pure waves by means of homotopy-Padé technique. The curves c^2/c_0^2 versus the wave height H in case of $\epsilon = -0.25,\ -0.15,\ 0,\ 0.25$ and 0.5 are shown in Fig. 6. Note that the $[8,8]$ and $[12,12]$ homotopy-Padé approximations agree quite well, except for a few points very close to the highest wave. In comparison with pure waves ($\epsilon = 0$), the aiding exponential shear currents ($\epsilon < 0$) tend to enlarge the wave phase velocity for given wave height H, but the opposing exponential shear currents ($\epsilon > 0$) tend to shorten it. Especially, as shown in Table 3 and Fig. 7, the

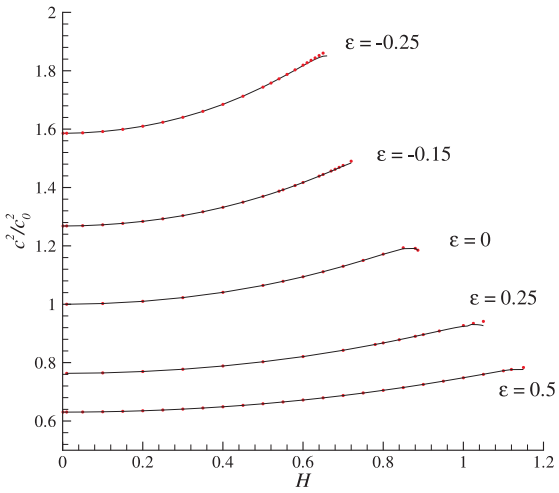

Figure 6. The dispersion relationship of waves on a current with an exponential distribution of vorticity $\Omega = \epsilon \exp(-\psi)$ in case of $\epsilon = -0.25,\ -0.15,\ 0,\ 0.25,\ 0.5$. Solid line: $[12, 12]$ homotopy-Padé approximation; Symbols: $[8, 8]$ homotopy-Padé approximation.

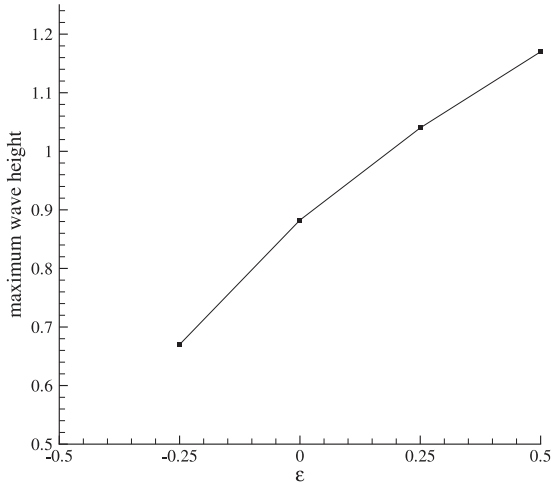

Figure 7. The maximum wave height versus ϵ in case of shear currents.

maximum wave heights are different for different currents: the aiding exponential shear currents ($\epsilon < 0$) tend to shorten the maximum wave height, but the opposing exponential shear currents ($\epsilon > 0$) tend to enlarge it. Note that, the maximum wave height of propagating waves on still water is about $H = 0.8825$. However,

in case of the opposing exponential shear currents ($\epsilon > 0$), the wave height can be greater than the limiting value for pure waves, as shown in Table 3 and Fig. 7. For example, in case of the opposing exponential currents with $0.25 \leq \epsilon \leq 0.5$, we obtain convergent series solutions of horizontal velocity u under the crest and trough of waves with $H = 0.92$, which is even higher than $H = 0.886$ given by Stokes theory for pure waves on still water (see [37]), as shown in Fig. 8. It should be emphasized that, according to Stokes theory, the propagating wave with $H = 0.92$ can *not* exist for pure waves on still water ($\epsilon = 0$). However, in case of the opposing shear current with $\epsilon = 0.25$, we get the convergent series solution of waves even with $H = 1.02$, as shown in Fig. 9. Thus, according to our results, the maximum wave height of propagating water waves on an opposing shear current ($\epsilon > 0$) can be larger than that of pure waves on still water. Note that the wave shape in case of $H = 1.02$ and $\epsilon = 0.25$ is steeper even than that of waves on still water with $H = 0.8825$, as shown in Fig. 9.

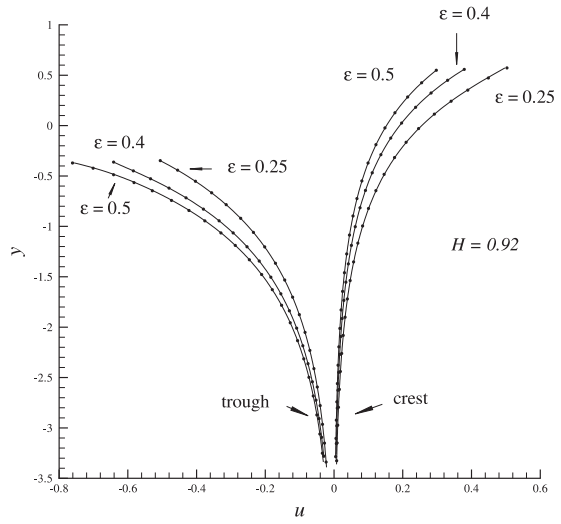

Figure 8. Approximations of horizontal velocity u under crest and trough of waves on different exponential opposing currents in case of $H = 0.92$ by means of $\hbar = -1/2$. Solid line: the 25th-order approximation; Dotted line: the 20th-order approximation.

As suggested by Stokes [1, 2], a train of propagating waves on still water breaks when the fluid velocity at crest is equal to the wave phase speed. To check this criteria for waves on a shear current, we also calculate the kinetic energy of the flow particle at crest in the reference frame moving with speed c, defined by

$$KE_c = \frac{1}{2}\,\boldsymbol{u}^2 = \frac{1}{\delta}[\kappa - y(0,0)]. \tag{53}$$

Physically, KE_c must be a non-negative value. The curves of KE_c versus the

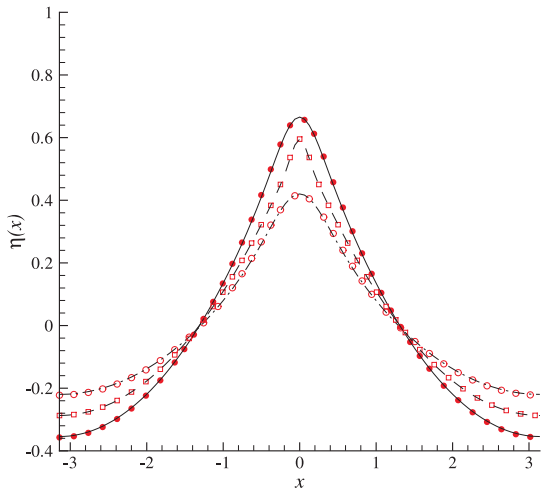

Figure 9. Approximations of wave elevation by means of $\hbar = -1/2$. Solid line: 25th-order approximation in case of $H = 1.02$ and $\epsilon = 0.25$; Dashed line: 45th-order approximation in case of $H = 0.8825$ and $\epsilon = 0$; Dot-dashed line: 25th-order approximation in case of $H = 0.64$ and $\epsilon = -0.25$; Circles: the corresponding 20th-order approximations; Square: the corresponding 40th-order approximation.

wave height H in case of the aiding current ($\epsilon = -0.25$), still water ($\epsilon = 0$) and the opposing current ($\epsilon = 0.25$) are shown in Fig. 10. Note that $KE_c \approx 0$ when $H \approx 0.8825$ for waves on still water ($\epsilon = 0$), which basically agrees with the results of the highest wave given by Schwartz [38] and Longuet–Higgins [39]. However, $KE_c \approx 0$ when $H \approx 0.67$ for waves on an aiding current ($\epsilon = -0.25$), and when $H \approx 1.04$ for waves on an opposing current ($\epsilon = -0.25$), respectively. So, it seems that the highest wave indeed corresponds to $KE_c = 0$, i.e. the fluid velocity at crest equals the wave phase speed. Note that the three curves of $KE_c \sim H$ in case of $\epsilon = \pm 0.25$ and $\epsilon = 0$ seem approximately parallel. So, although the results for the highest waves are not so accurate as those of waves with smaller amplitude, we are quite sure that, qualitatively speaking, an aiding shear current tends to shorten the maximum wave height, but an opposing shear current has an opposite effect. This conclusion also agrees with the experiment made by Dr. Xu [40], who observed that waves on an aiding current break with lower wave height than waves on still water in the Shanghai Jiao Tong University State Key Laboratory of Ocean Engineering. Therefore, according to our analytic results, Stokes' criteria of wave breaking still holds for waves on the non-uniform current: a train of propagating waves on a shear current breaks as the fluid velocity at crest equals the wave phase speed.

Wave shapes at crest and trough in case of $H = 0.3$ and $-0.25 \leq \epsilon \leq 0.25$ are shown in Figs. 11 and 12. It is found that, for given wave height H, the aiding exponential shear current tends to sharpen the crest but smoothen the trough, and

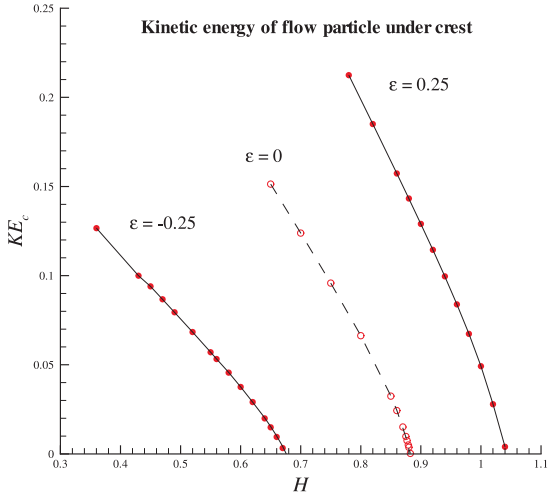

Figure 10. The kinetic energy KE_c of flow particle at crest versus the wave height H. Filled circles: $[11, 11]$ homotopy-Padé approximation; Solid line: $[12, 12]$ homotopy-Padé approximation; Open circles: $[15, 15]$ homotopy-Padé approximation; Dashed line: $[20, 20]$ homotopy-Padé approximation.

the opposing shear current has the opposite effect. This might partly explain why the aiding exponential shear current tends to shorten the maximum wave height but the opposing one tends to enlarge it. Note that the wave shape on a uniform current is the same as that on still water. Therefore, it is not the magnitude but the non-uniformity of the current that has great influence on the wave shape of propagating waves.

The horizontal velocity profiles $u - u_c$ under wave crest and trough on the same stream lines in case of $H = 0.3$ and $-0.25 \leq \epsilon \leq 0.25$ are shown in Fig. 13, where u is the whole horizontal velocity of wave-currents, and u_c denotes the velocity of the pure current (in case of $H = 0$). For waves on still water ($\epsilon = 0$), the horizontal velocity under crest is in the same direction as wave propagation, but the horizontal velocity under trough is in the opposing direction. For waves on an shear current, it is found that the aiding current tends to shorten the horizontal velocity under crest and trough, while the opposing current has the opposite effects, as shown in Fig. 13. Besides, the horizontal velocity of waves on an aiding current delays more quickly over the depth than that of waves on an opposing current. Furthermore, the larger the vorticity of the shear current, the larger the influence of the current on the horizontal velocity, as shown in Fig. 13. Finally, it should be pointed out that the maximum absolute value of u_i caused by the wave-current interaction is not on the wave surface but beneath it.

It is well-known that the amplitude of propagating waves on still water ($\epsilon = 0$) decays exponentially over the depth. The amplitude of waves on a shear current,

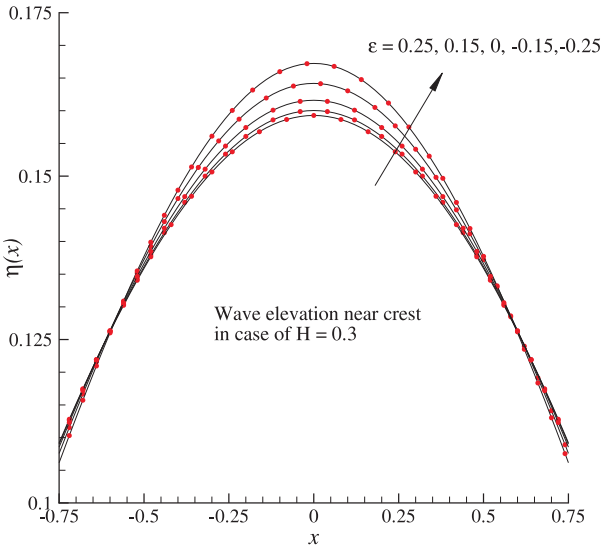

Figure 11. Wave elevations near the crest in case of $H = 0.3$ and $-0.25 \leq \epsilon \leq 0.25$ by means of $\hbar = -1/2$. Solid line: the 25th-order approximation; Circles: the 20th-order approximation.

given by

$$A_w(\psi) = y(0, \psi) - y(\pi, \psi), \tag{54}$$

is investigated here. The curves of $A_w \sim \psi$ in case of $H = 0.3$ and $-0.25 \leq \epsilon \leq 0.25$ are shown in Fig. 14, which indicates that the amplitude of propagating waves on an aiding shear current decays over the depth more quickly than that of waves on an opposing one. This agrees with the conclusion mentioned in the above paragraph that the horizontal velocity of the waves on an aiding current delays more quickly over the depth than that of waves on an opposing current. Thus, in case of bad weather condition at sea, a submarine or a Remote Operated Vehicle (ROV) or a Autonomous Underwater Vehicles (AUV) on an aiding shear current should be safer than that on still water or an opposing shear current. In other words, a submarine or a ROV or a AUV on an opposing shear current is more dangerous than that on still water.

5. Conclusions

In this paper, an analytic method for strongly nonlinear problems, namely the homotopy analysis method (HAM) [17, 20, 19, 22], is employed to get convergent series solutions of the nonlinear propagating water waves on a shear current which possesses an exponential distribution of vorticity. By means of Dubreil–Jacotin

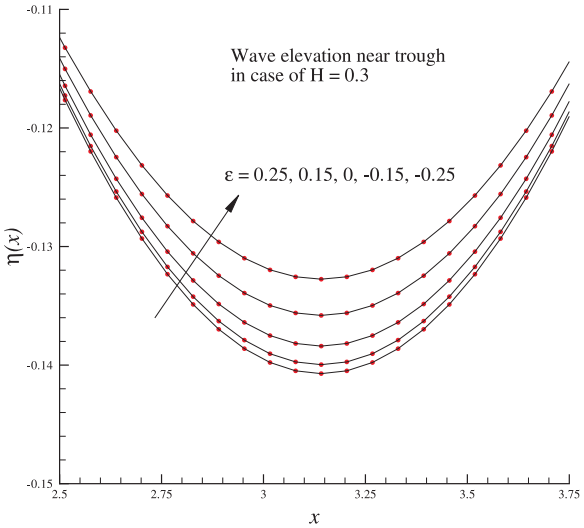

Figure 12. Wave elevations near the trough in case of $H = 0.3$ and $-0.25 \leq \epsilon \leq 0.25$ by means of $\hbar = -1/2$. Solid line: the 25th-order approximation; Circles: the 20th-order approximation.

transformation, the original exponentially nonlinear governing equation subject to the nonlinear boundary conditions on an unknown free surface is reformulated into an algebraically nonlinear governing equation with the nonlinear boundary conditions satisfied on a known boundary. So, the Dubreil–Jacotin transformation greatly simplifies resolving this problem. By means of the homotopy analysis method, this kind of nonlinear boundary value problem is further transferred into an infinite number of linear subproblems within a known domain, which can be solved easily by means of symbolic computation softwares. Accurate high-order approximations are obtained for not only small amplitude waves a weak current but also large amplitude waves on a rather strong current. Note that the perturbation solutions are valid only for small amplitude waves on a current with weak vorticity. For waves with large amplitude or waves on a current with comparatively strong vorticity, the perturbation solutions mostly overestimate the wave speed, as shown in Figs. 3 to 5. This shows the great potential of the homotopy analysis method for the complicated nonlinear problems. Obviously, it is straightforward to apply this approach to investigate propagating waves on non-uniform currents with more complicated vertical distributions of vorticity.

Mathematically, it should be emphasized that the auxiliary linear operators (22) and (23) can have nearly no relationships with the original equations (8) and (9). Different from all other analytic techniques which are often strongly dependent upon linear operators in the original governing equations, the homotopy analysis

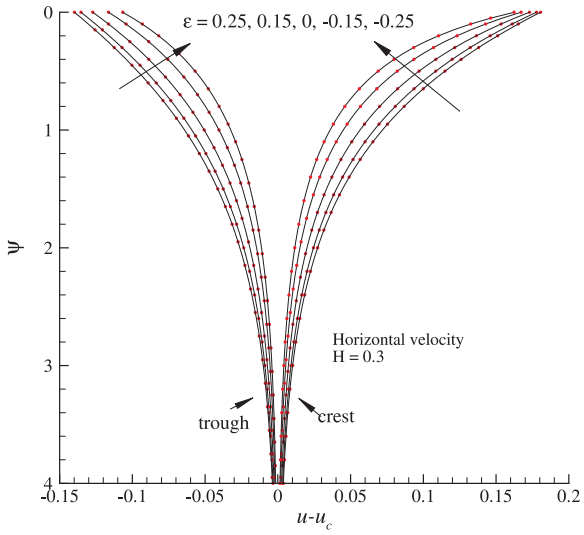

Figure 13. Influence of currents on horizontal velocity profiles of propagating waves in case of $H = 0.3$ and $-0.25 \leq \epsilon \leq 0.25$ by means of $\hbar = -1/2$. Solid line: the 25th-order approximation; Symbols: the 20th-order approximation.

method provides us great freedom to choose the auxiliary linear operators by means of analyzing the physical background of the considered problem. So, by means of the homotopy analysis method, we need not spend too much time in the form of a nonlinear equation, but should pay more attention to its physical background so as to find a proper solution expression. This is in principle quite different from other analytic techniques, as pointed out by Liao and Tan [22]. Note that, it is the homotopy analysis method which provides us with, for the first time, such kind of freedom which can greatly simplify resolving nonlinear problems, not only analytically but also numerically, as shown in this paper and also illustrated in [22]. So, mathematically, this analytic method is rather general in principle and can be employed to solve many types of nonlinear partial differential equations with variable coefficients in science, finance and engineering.

Physically, the influences of an exponential shear current on a train of waves are investigated in detail. It is found that, for given wave amplitude, waves propagate faster on an aiding shear current but more slowly on an opposing one, compared with waves in still water. Besides, different from the uniform current, an aiding shear current tends to sharpen the crest but smoothen the trough, while an opposing shear current has the opposite effects. So, it is not the magnitude but the nonuniformity of the current that influences the wave shape. Furthermore, the amplitude of waves and fluid velocity decay over the depth more quickly on an aiding shear current but more slowly on an opposing shear current than that of waves in still water. Especially, it is found that Stokes' criteria of wave breaking

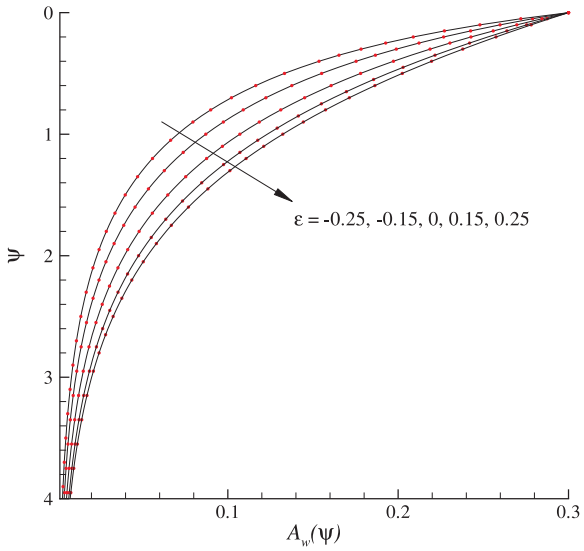

Figure 14. The decay of wave amplitude in case of $H = 0.3$ and $-0.25 \leq \epsilon \leq 0.25$ by means of $\hbar = -1/2$. Solid line: the 25th-order approximation; Symbols: the 20th-order approximation.

still holds for waves on a non-uniform current, and the highest wave on an opposing shear current is even higher and steeper than that of waves on still water.

Finally, to show the importance of this work in practice, it should be pointed out that the small percentage changes of horizontal velocities of fluid result in twice as large changes in drag forces on offshore structures, and the deck elevation of offshore structures is dependent on the knowledge of crest elevation [3].

Acknowledgement

Thanks to Prof. Roger Grimshaw for the suggestive discussions and the anonymous reviewers for their valuable comments. This work is partly supported by National Natural Science Foundation of China (Approval No. 10572095 and 50739004), Program for Changjiang Scholars and Innovative Research Team in University (Approval No. IRT0525), and National 863 Plan Project of China (Approval No. 2006AA09Z354).

References

[1] Stokes, G. G., Supplement to a paper on the theory of oscillatory waves. *Math. Phys. Papers* **1** (1880), 314–326.

[2] Stokes, G. G., On the theory of oscillation waves. *Trans. Cambridge Phil. Soc.* **8** (1894), 441–455.
[3] Dalrymple, R. A., A numerical model for periodic finite amplitude waves on a rotational fluid. *J. Comput. Phys.* **24** (1977), 29–42.
[4] Fenton, J. D., A fifth-order Stokes theory for steady waves. *J. Waterw. Port Coastal and Ocean Eng.* **111** (1985), 216–234.
[5] Clamond, D., Steady finite-amplitude waves on a horizontal seabed of arbitrary depth. *J. Fluid Mech.* **398** (1999), 45–60.
[6] Clamond, D., Cnoidal-type surface waves in deep water. *J. Fluid Mech.* **489** (2003), 101–120.
[7] Clamond, D. and Fructus, D., Accurate simple approximation for the solitary wave. *C. R. Mecanique* **331** (2003), 727–732.
[8] Thompson, P. D., The propagation of small surface disturbances through rotational flow. *Ann N Y Acad Sci* **51** (1949), 463–474.
[9] Kishida, N. and Sobey, R. J., Stokes theory for waves on linear shear current. *J. Waterw. Port Coastal and Ocean Eng.* **114** (1988), 1317–1334.
[10] Eastwood, J. W. and Watson, C. J. H., Implication of wave-current interaction for offshore design. *E and P Forum,Paris* (1989).
[11] Peregrine, D. H., Interaction of water waves and current. *Adv. Appl. Mech.* **16** (1977), 9–117.
[12] Toumazis, A. D. and Ahilan, R. V., Review of recent analytical and approximate solutions of wave-current interaction. *Enviromental forces on offshore strucure and their prediction* **26** (1990), 61–79.
[13] Wang, T. and Li, J. C., On wave-current interaction. *Adv. in Mech.* **29(3)** (1999), 331–343.
[14] Thomas, G. P., Wave-current interactions: an experimental and numerical study. Part 2. Nonlinear waves. *J. Fluid Mech.* **216** (1990), 505–536.
[15] Li, J. C. and Chwang, A. T., Effects of nonuniform current on the wave field. *Proc. of 4th Inter Offsh. and Polar Eng. Conf. Osaka*, **3** (1994), 125–132.
[16] Wang, T. and Li, J. C., Effect of nonlinear wave-current interaction on flow fields and hydrodynamic forces. *Science in China*, Ser A, **40(6)** (1997), 622–632.
[17] Liao, S. J., *The proposed homotopy analysis technique for the solution of nonlinear problems.* PhD thesis, Shanghai Jiao Tong University, 1992.
[18] Liao, S. J., An explicit, totally analytic approximation of Blasius viscous flow problems. *Int. J. of Non-Linear Mech.* **34(4)** (1999), 759–778.
[19] Liao, S. J. and Cheung, K. F., Homotopy analysis of nonlinear progressive waves in deep water. *Journal of Engineering Mathematics* **45(2)** (2003), 105–116.
[20] Liao, S. J., *Beyond Perturbation: Introduction to the Homotopy Analysis Method.* Chapman & Hall/ CRC Press, Boca Raton 2003.
[21] Liao, S. J., On the homotopy analysis method for nonlinear problems. *Applied Mathematics and Computation* **147** (2004), 499–513.
[22] Liao, S. J., Tan, Y., A general approach to obtain series solutions of nonlinear differential equations. *Studies in Applied Mathematics* **119** (2007), 297–254.
[23] Abbasbandy, S., Soliton solutions for the 5th-order KdV equation with the homotopy analysis method. *Nonlinear Dynamics* **51** (2008), 83–87.
[24] Tao, L., Song, H. and Chakrabarti, S., Nonlinear progressive waves in water of finite depth – an analytic approximation. *Coastal Engineering* **54** (2007), 825–834.
[25] Yamashita, M., Yabushita, K. and Tsuboi, K., An analytic solution of projectile motion with the quadratic resistance law using the homotopy analysis method. *J. of Physics A* **40** (2007), 8403–8416.
[26] Hayat, T. and Sajid, M., On analytic solution for thin film flow of a forth grade fluid down a vertical cylinder. *Physics Letters A* **361** (2007), 316–322.
[27] Allan, F. M., Derivation of the Adomian decomposition method using the homotopy analysis method. *Applied Mathematics and Computation* **190** (2007), 6–14.

[28] Bataineh, A. S., Noorani, M. S. M. and Hashim, I., Solutions of time-dependent Emden-Fowler type equations by homotopy analysis method. *Physics Letters A,* **371** (2007), 72–82.
[29] Zhu, S. P., An exact and explicit solution for the valuation of American put options. *Quantitative Finance* **6** (2006), 229–242.
[30] Abbasbandy, S., The application of the homotopy analysis method to nonlinear equations arising in heat transfer. *Physics Letters A* **360** (2006), 109–113.
[31] Alizadeh-Pahlavan, A., Aliakbar, V., Vakili-Farahani, F. and Sadeghy, K., MHD flows of UCM fluids above porous stretching sheets using two-auxiliary-parameter homotopy analysis method . *Communications in Nonlinear Science and Numerical Simulation.* (online).
[32] Molabahrami, A. and Khani, F. The homotopy analysis method to solve the Burgers-Huxley equation. *Nonlinear Analysis B: Real World Applications.* (online).
[33] Wu, Y. and Cheung, K. F., Explicit solution to the exact Riemann problems and application in nonlinear shallow water equations. *Int. J. Numerical Methods in Fluids.* (online).
[34] Dubreil-Jacotin, M. L., Sur la détermination rigoureuse des ondes permanentes périodiques d'ampleur finie. *J. Math. Pures et Appl.* **13** (1934), 217–291.
[35] Drennan, W. M, Hui, W. H. and Tenti, G., Accurate calculations of Stokes water waves of large amplitude. *J. App. Math. Phys. (ZAMP)* **43** (1992), 367–384.
[36] Phillips, O. M. *The dynamics of the upper ocean.* Cambridge Press, 1977.
[37] Marshall, P., Tulin and Jiyue J. Li, On the breaking of energetic waves. *Int. J. Offshore Polar Eng.* **2(1)** (1992), 46–53.
[38] Schwartz, L. W., Computer extension and analytic continuation of Stokes' expansion for gravity waves. *J. Fluid Mech.* **62** (1974), 553–578.
[39] Longuet-Higgins, M. and Tanaka, M., On the crest instabilities of steep surface waves. *J. Fluid Mech.*, **336** (1997), 51–68.
[40] Xu, H., *Applications of the homotopy analysis method in fluid mechanics and ocean engineering.* PhD thesis, Shanghai Jiao Tong University, 2006.

Jun Cheng, Jie Cang and Shi-Jun Liao
State Key Lab of Ocean Engineering
School of Naval Architecture, Ocean and Civil Engineering
Shanghai Jiao Tong University
Shanghai 200030
China

(Received: April 25, 2007; revised: March 11, 2008)

Published Online First: October 10, 2008

To access this journal online:
www.birkhauser.ch/zamp